Synthesis of Sn-silicalite from hydrothermal synthesis of SiO_2-SnO_2 xerogels

Rafael van Grieken, Carmen Martos, Manuel Sánchez-Sánchez, David P. Serrano, Juan A. Melero,* José Iglesias and Alvar G. Cubero

Department of Chemical and Environmental Technology, ESCET, Universidad Rey Juan Carlos, C/ Tulipán s/n, 28933 Móstoles, Madrid, Spain

Published on:

Microporous Mesoporous Mater. 119 (2009) 176-185

doi:10.1016/j.micromeso.2008.10.020

* To whom correspondence should be addressed.

juan.melero@urjc.es

Ph. +34 91 488 7087. Fax +34 91 488 7068

Abstract

For the first time, the synthesis of Sn-zeolites starting from SiO_2-SnO_2 xerogels is described. The influence of several synthesis parameters in the physical-chemical properties of the xerogels and the zeolites subsequently generated has been investigated. Two different tin sources were assayed in the synthesis of xerogels (anhydrous $SnCl_4$ and $SnCl_4 \cdot 5H_2O$) as well as two gelation agents (NH_3 and TPAOH). Though both bases led SiO_2-SnO_2 xerogels mainly showing tetrahedrally coordinated tin centres, regardless the tin source, only TPAOH derived materials were easily transformed into MFI-type zeolites showing tin incorporation. On the other hand, NH_3 gelified xerogels were difficult to crystallize, being this fact attributed to the retention of NH_3 species in the xerogels because of the tin Lewis acidity, avoiding its inclusion in the zeolite crystalline framework. Studies on the crystallization time and temperature allowed to optimize the transformation of TPAOH gelified SiO_2-SnO_2 xerogels into tin-containing MFI zeolites showing isomorphically incorporated tin centres. The so-obtained materials were compared with conventionally synthesized SnS-1 zeolite showing better quality in terms of tin incorporation.

Keywords: Tin, Xerogels, Crystallisation, SnS-1, MFI.

1. Introduction

The interest of tin incorporation into zeolites dates from decades ago [1]-[3]. In these first articles, the substitution of Si by Sn into zeolite frameworks, particularly in MFI materials, was supported by different characterization techniques. However, their catalytic activity was not relevant as they were not probably tested in the appropriate reactions. In order to expand the applicability range of these tin-contining materials, zeolite structures with higher pore size, like Sn-β and Al-free Sn-β, were prepared and tested in the oxidation of aromatic compounds [4]. A few years later, the report of the excellent catalytic behaviour of analogue Sn-contaning beta zeolites in Baeyer Villiger reaction [5] – with practically 100% conversion and 100% selectivity for certain subtracts – renewed the interest on tin-functionalized zeolites and related materials [6]-[11].

Sn-beta zeolite is difficult to synthesize since it seems not to spontaneously crystallise from Sn-contained gels. This is overcome by the addition of some seeds of nano-crystalline pure-

silica beta to the gel [5], being therefore essential two proper syntheses of the two BEA-structured materials, with and without tin atoms. The incorporation of tin into BEA framework by this method is limited to a Si/Sn ratio higher than 120 [11],[12], probably as a consequence of the substitution of Sn atoms in the BEA framework is an endothermic process [13]. Higher Sn content into the gel implies the presence of undesired extra-framework Sn species in the final samples.

Similar problems were described for the incorporation of Ti in zeolites. Their catalytic activity was found to depend on the amount of isomorphically substituted Ti into the zeolite framework [14],[15]. The incorporation of Ti into MFI-structured zeolites was found to be limited to a particular content, regardless the synthesis method [16],[17]. In this context, the preparation of zeolite TS-1 from wetness impregnated SiO_2-TiO_2 xerogels was proposed as an alternative [18] since, unlike the conventional crystallization of zeolites, its transformation from xerogels is given by a solid-solid mechanism [19],[20]. Ti (and also Sn [21]) substitution limit in xerogels is very much higher than that in zeolites [22], because the former does not force the metal to occupy a particular spatial position. On the other hand, there is not doubt about the chemical similarities of Sn^{4+} and Ti^{4+}. For instance, both are the most stable oxidation state of their atoms in aqueous solution, and both corresponding oxides have rutile-like topology. Moreover, the incorporation of both ions into the zeolite framework produces similar electronic properties since they are equally interpreted by Diffuse-Reflectance UV-Vis (DR-UV-Vis) and Fourier Transform Infrared (IR) spectroscopies [23].

Herein we present the first study of the transformation of SiO_2-SnO_2 xerogels into Sn-zeolites. In particular, this work is focused on MFI, the topology being studied in the transformation of xerogels in zeolites.

2. Experimental

Synthesis of the materials

SiO_2-SnO_2 xerogels were prepared by a two-step sol-gel method. Tetraethylorthosilicate (TEOS) and either $SnCl_4$ (previously dissolved in freshly-distilled anhydrous ethanol in a dry box) or soluble-in-water $SnCl_4 \cdot 5H_2O$ were added to a 0.05 M HCl aqueous solution and partially hydrolysed for one hour under stirring. The two-phase mixture becomes a unique phase after five minutes under agitation. Next, an aqueous base (NH_4OH 1 M or TPAOH 20

wt%) is dropwise added until the gel point is reached. The so-formed gel is dired at 110 ºC becoming a xerogel.

The resultant xerogels were wetness impregnated with TPAOH (1.6 g per 1 g of xerogel) [20] and the mixture were hydrothermally treated at different crystallisation temperatures (150-190 ºC) for different times (1-30 days). The solids were washed and dried at 110 ºC overnight. Finally, the samples were calcined at 550 ºC under air atmosphere for 5 hours to remove the template.

The samples will be named as follows: the xerogels will be identified with letter X followed by a number representing the content of Sn, being 3, 6 and 9 wt%; in the case of zeolites, their names starts with Z followed by a number, only indicating an arbitrary order.

Characterisation techniques

Phase purity of the samples was checked by X-ray diffraction (XRD). XRD patterns were acquired on a Philips X'PERT MPD diffractometer using Cu Kα radiation. Crystallinity of Sn-zeolites with MFI topology was calculated from the area below the curve in the range 22.4-24.7º, referenced to the same reflections of the XRD pattern of a silicalite-1 sample, considered as 100 % crystalline, which was prepared from a pure silica xerogel. The tendencies in crystallinity were corroborated by the intensity variations of the double five-ring lattice vibration band at ca. 550 cm^{-1} in the FT-IR spectra [24].

DR-UV-Vis spectra were recorded on a Varian CARY-500 spectrophotometer equipped with a diffuse reflectance accessory in the wavelength range from 200 to 600 nm. A halon white reflectance standard was used as a reference material.

Tin content was determined by ICP-atomic emission spectroscopy. The samples (100 mg) were dissolved in aqueous hydrofluoric acid. After dissolution, the samples were diluted in water until filling a 1 L calibrated flask. An absorption standard solution of Sn (1000 μg ml^{-1} in water) was used for the calibration of the equipment.

Scanning electron microscopy (SEM) images and micro-elemental analysis (EDX) were carried out on a XL30 ESEM Philips, operating at 30 kV.

Thermogravimetric analysis (TGA) were performed in N_2 flow on a TA instrument SDT 2960 thermobalance, with a heating rate of 5ºC·min^{-1} up to 800ºC.

FT-IR spectra of fresh catalysts were recorded on a Mattson Infinity Series spectrophotometer using the potassium bromide wafer technique.

^{119}Sn magic-angle spinning nuclear magnetic resonance (MAS NMR) spectra were recorded using a Varian Infinity-400 spectrometer (9.4 T) at 149.0 MHz, using a 7-mm probe. Spinning rates of 6 KHz, pulse lengths of 1.7 μs (π/4) and pulse delays of 40 seconds were applied. ^{119}Sn chemical shifts were referenced against tetramethyl tin, taken as 0 ppm.

Acidity of the samples was determined by ammonia temperature programmed desorption (TPD) in a Micromeritics 2910 (TPD/TPR) equipment. The calcined samples were outgassed under a helium flow (50 Nml·min^{-1}) with a heating rate of 15 ºC·min^{-1} up to 560ºC and kept at this temperature for 30 min. After cooling to 60 ºC, an ammonia flow of 35 Nml·min^{-1} was passed through the sample for 30 min. The physisorbed ammonia was removed by flowing helium at 60 ºC for 90 min. The chemically adsorbed ammonia was determined by increasing the temperature up to 550 ºC with a heating rate of 15 ºC·min^{-1}, maintaining afterwards this temperature for additional 30 min. The ammonia concentration in the effluent stream was measured through a thermal conductivity detector. Acidity of the samples were quantified by comparing the area of the TPD bands with that of a zeolite Al-ZSM-5 (Si/Al=30), considering that every Al atom is incorporated into the zeolite framework generating a Brönsted acid site.

3. Results and discussion

Xerogels

Figure 1 shows the DR-UV-Vis spectra of xerogels prepared with either anhydrous or $SnCl_4$ pentahydrate for three different tin contents. All of them were gelified with a 1 M aqueous solution of NH_4OH. Regardless the Sn source, it is evident that Sn is mainly tetrahedrally coordinated and scarce contribution of Sn species with higher coordination, if any, is detected. Therefore, there is not a discernible effect of the nature of the tin source on the tin coordination in the SiO_2-SnO_2 xerogels. Other physical-chemical properties of the xerogels prepared with different tin sources were studied by an exhaustive characterization study including techniques such as chemical analysis by ICP-AES, TGA, N_2 adsorption-desorption isotherms at 77 K, FT-IR spectroscopy, and NH_3-TPD (results not shown). Significant differences between xerogels were not found in any of these techniques, except the TGA weight loss of NH_3 is observed at higher temperatures in the xerogels prepared with

anhydrous tin source (254 ºC for a xerogel containing 3 wt. % of Sn) than in those prepared with $SnCl_4 \cdot 5H_2O$ (233 ºC for a xerogel with the same tin content). Because of the experimental simplicity in preparing xerogels with the soluble-in-water $SnCl_4 \cdot 5H_2O$ and especially because their better transformation to zeolites MFI (see below), pentahydrate tin chloride will be the precursor of the SiO_2-SnO_2 xerogels discussed from now on, unless other thing will be stated.

DR-UV-Vis spectra shown in Figure 1 also evidences that tin coordination does not vary with the Sn content, at least in the studied range 3-9 wt. % of Sn, for any of both Sn sources. ICP-AES analyses confirmed that all Sn and all Si are found in the final xerogels. The homogeneity in tin coordination is additionally supported by ^{119}Sn MAS NMR studies (Figure 2). The ^{119}Sn NMR spectra of the xerogels with 3 and 9 wt. % of Sn prepared with $SnCl_4 \cdot 5H_2O$ are dominated by a broad but symmetrical signal without any other significant contribution. The large width of the signal must be related with the amorphous nature of the xerogel, which would provide a wide distribution of environments for a given Sn coordination. The main difference between the ^{119}Sn NMR spectra of the xerogels with different tin content seems to be the intensity of that resonance. More importantly, the ^{119}Sn chemical shift of this signal is centred at *ca.* -688 ppm, very different from the δ ^{119}Sn of SnO_2 (-605 ppm) and very similar to that of hydrated Sn-beta [12], Sn-MFI [25], Sn-MEL [3] and Sn-MCM-41 [26], which where assigned to tetrahedral, octahedral and even penta-coordinated Sn, but located into the framework in any case. The high Sn content able to be incorporated into the SiO_2 matrix of a xerogel (at least, 9 wt. % of Sn, that is, Si/Sn ratio of 19.4) as it is deduced from DR-UV-Vis and ^{119}Sn MAS NMR, supports our hypothesis about a minor restriction to accommodate tin in xerogels compared the crystalline zeolite.

Figure 3A shows the FT-IR spectra of the xerogels containing 0, 3, 6 and 9 % wt. of Sn and gelified with NH_4OH, whereas Figure 3B contains the TGA plots of the same samples. Basically, all FT-IR spectra have the same bands, although the intensity of some of them systematically changes with the increase of Sn content. All spectra contain a band at *ca.* 1635 cm^{-1} with similar relative intensity. It is characteristic of water, especially when it is accompanied by a very broad band in the –OH region (3100-3700 cm^{-1}), just like in the shown spectra. However, there is an increase of the relative intensity of the band at *ca.* 960 cm^{-1}. In spite of the origin of this band has been widely discussed in the literature [27],[28], it is not completely clear but it is accepted as a good indication of the presence of bonds Si-O-M (where M represents a heteroatom) in SiO_2 frameworks. The FT-IR spectrum of our Sn-free

xerogel also shows evidences of that signal (maybe due to the presence of groups SiO^- [28]), but it is very much clearer in the xerogels containing tin, suggesting again the chemical integration of tin into the SiO_2 matrix.

The IR bands at *ca.* 3185 and 1410 cm^{-1}, which are basically absent in the FT-IR spectrum of the xerogel X0, increase their intensity from the spectra of the xerogel X3 to that of the X9. These bands were attributed to the stretching and bending vibrations of NH_3, respectively. Since there is a complete absence of these bands in the spectra of X0, the NH_3 molecules are presumably retained by the Sn^{4+} ions, indicating that they may be Lewis acid centres. The TGA curves (Figure 3B) of the xerogels containing Sn, possess a weight loss at temperatures higher than 250 ºC, which evidently cannot be assigned to adsorbed H_2O, and therefore it must be due to adsorbed NH_3. Indeed, that weight loss increases with the Sn content of the xerogels. The analysis of the first derivative curve of weight gives additional information from the temperature region at which NH_3 is lost. The maximum of that weight loss is systematically shifted to higher temperatures for Sn-richer xerogels. Moreover, the presence of more than one weight loss becomes evident in the TGA derivative of the Sn-richest xerogels. These features could be related to Lewis acid centres of different strength. Such heterogeneity in the acidity provided by incorporated tin in SiO_2 framework has been described even in Sn-beta [29], where the crystalline restrictions should reduce the potential versatility of environments.

In order to properly study the acidity of the xerogels with different Sn content, we carried out TPD analysis of ammonia (Figure 4). Unlike xerogel X0, which is practically unable to retain any amount of NH_3, the SiO_2-SnO_2 xerogels retain NH_3 with different strength. Moreover, also in good agreement with the TGA analyses, the xerogels with the highest tin content retains higher amount of NH_3 and at higher temperatures. This comparison should be considered in qualitative terms as the xerogels were treated at 560 ºC before TPD analyses whereas TGA measurements were directly carried out on the as-prepared samples. In any case, TPD supports the suggested heterogeneity in the acidity of the SiO_2-SnO_2 xerogels and their subsequent affinity for NH_3.

The presence of significant amount of NH_3 at such high temperatures in the SiO_2-SnO_2 xerogels could retard the crystallization of Sn-silicalite. That is the reason why we investigated the preparation of the xerogels gelified with TPAOH, which is the most extensively used structure-directing agent for MFI-structured zeolites, giving good results in the transformation of xerogels SiO_2-TiO_2 to TS-1 [20]. Figure 5A and Figure 5B show the

DR-UV-Vis spectra and the TGA plots, respectively, recorded for two SiO_2-SnO_2 xerogel with 3 wt. % of Sn, gelified with TPAOH and with NH_4OH. DR-UV-Vis spectroscopy clearly shows that Sn with tetrahedral coordination can mainly be afforded also with TPAOH as gelificant agent. On the other hand, a higher weight of gelificant agent was found in the xerogel containing TPAOH by TG analyses. Unlike the undoubted retention of NH_3 by the Sn centres, TPAOH could simply be retained on the xerogel because of its low volatility and also because strong adsorption over the tin centres. However, the molar ratio TPAOH/Sn in this xerogel is lower than NH_3/Sn in the xerogel gelified with ammonia, both calculated by TG experiments. Nevertheless, the retention of TPA^+ cations on SiO_2-SnO_2 xerogels should not exert negative influence on the transformation of the same into Sn-silicalite, since TPA^+ is the typically structure directing agent used for the preparation of MFI zeolites and it is indeed added to these xerogels during the impregnation procedure before the crystallization step.

Zeolites

Every experiment dealing with the transformation of xerogels into zeolites presented in this section has been carried out starting from SiO_2-SnO_2 xerogels containing 3 wt. % of Sn, excepting pure-SiO_2 MFI obtained by the TPAOH impregnation of xerogel X0. Table 1 shows the experimental conditions of some relevant attempts to get Sn-silicalite from SiO_2-SnO_2 xerogels. In all experiments indicated in Table 1, a crystallisation time of 13 days were used. Some amount of MFI phase was found in every single attempt, which was the only crystallised phase.

Some different parameters with potential influence on the kinetics of formation of MFI materials from SiO_2-SnO_2 xerogels were systematically changed. Thus, in the experiments Z1-Z3, the influence of crystallization temperature was studied in the 150-190ºC range, following the temperature range investigated in the literature for transformation of SiO_2-TiO_2 xerogels into TS-1 [20]. Both XRD patterns and DR-UV-Vis spectra of these three samples are shown in Figures 6A and 6B, respectively. In spite of the very long crystallization time (13 days), the activation energy given by the hydrothermal treatment at 150 and 170ºC is clearly not enough to get crystalline samples from these xerogels. Only when temperature is as high as 190ºC, an acceptable MFI crystallinity is afforded. It strongly contrasts with the kinetics of crystallization of silicalite-1 from Sn-free xerogel X0, which was completely transformed into a crystalline pure-SiO_2 MFI material after a few hours (its XRD pattern was

indeed taken as 100 % reference for the crystallinity calculation of the Sn-silicalite samples). This fact suggests that the presence of tin in the starting xerogel have an inhibitor effect on the kinetics of MFI crystallization. It could be related with the above-mentioned inability of Sn-beta to spontaneously crystallise and the limited Sn incorporation in its framework [5],[12]. Supporting this reasoning, sample Z3, the unique crystalline one from Figure 6A, seems not to have tin incorporated in tetrahedral coordination, according to its DR-UV-Vis spectrum (Figure 6B) being this rather similar to that achieved for tin oxide used for reference purposes. Therefore, an increase of crystallization temperature has negative effects on Sn incorporation into the zeolite framework, although we must take into account that, since samples Z1 and Z2 are almost totally amorphous, the tetrahedral signal of DR-UV-Vis spectra will probably come from the non-transformed xerogel.

The comparison of the samples Z3 and Z4 has allowed to determine the influence of the Sn source on the kinetics of the xerogel-to-zeolite transformation. Accordingly to the above-shown characterisation results, this variable has practically negligible influence on the physico-chemical properties of the xerogels. However, Table 1 makes clear that, under the studied conditions, only xerogels prepared with $SnCl_4 \cdot 5H_2O$ as Sn source, and not those prepared with anhydrous $SnCl_4$, could be abundantly transformed into MFI-structured zeolite. The retarded effect on the transformation kinetics of the xerogels prepared with anhydrous tin chloride could be due to the stronger affinity of this xerogel to retain NH_3 (see above). In both samples the Sn incorporation into the zeolite framework deduced from the DR-UV-vis spectra (not shown) was far from being adequate.

The strong affinity of SiO_2-SnO_2 xerogels for NH_3, together with the experimental methods described in the literature about the transformation of SiO_2-TiO_2 xerogels into Ti-zeolites [18]-[20], led us to use TPAOH as gelificant agent in the preparation of SiO_2-SnO_2 xerogels. The fact that TPA^+ is retained at higher temperatures than NH_3 by similar SiO_2-SnO_2 xerogels has to be considered as an advantage rather than inconvenient since TPA^+ is the conventional SDA of MFI zeolites. Samples Z2 and Z5 were prepared under the same conditions from hydrothermal transformation of two xerogels, whose unique difference was the nature of the basic agent used in the gelation process, NH_3 or TPAOH (Table 1). The improvement in the MFI crystallinity when TPAOH was the gelificant agent is evident, supporting the negative effect on the kinetics of xerogel-to-zeolite transformation attributed to the NH_3 retained by the xerogel during the drying process.

Once $SnCl_4 \cdot 5H_2O$ and TPAOH were respectively selected as tin source and as gelificant agent in the preparation of SiO_2-SnO_2 xerogels, the kinetic study of the transformation of one of these xerogels into Sn-silicalite-1 at 170 ºC was carried out (synthesis conditions of samples Z5). Figure 7A depicts the XRD patterns of the samples resulting after the hydrothermal treatment of the TPAOH-impregnated SiO_2-SnO_2 xerogel for 1, 3, 6 and 13 days, which has been denoted as Z6A, Z6B, Z6C and Z6D, respectively. Figure 7B plots the crystallinity of those samples *versus* crystallisation time. Despite of being crystallised at 170 ºC, good crystalline MFI samples (87 %) were obtained after just one day of crystallisation, which could be surprising according to the information from Table 1. However, it must be noted that a xerogel gelified with TPAOH has been used and that the cristallinity reaches a maximum and then it decreases with crystallisation time. This behaviour supports the reduced crystallinity values of the samples crystallised from the xerogels gelified with TPAOH after 13 days given in Table 1. After 3 days of crystallization, a maximum of crystallinity is reached (95 %). From this point, the crystallinity decreases with the crystallization time. It is noteworthy this behaviour is just opposite to the trend of crystallinity for samples prepared from the hydrothermal treatment of xerogels gelified with NH_3 which is, apart from kinetically very much slower, always ascendant.

The existence of a maximum in the crystallinity with the crystallisation time suggests the instability of the formed zeolite after prolonged contact with the mother liquid under hydrothermal conditions. Figure 8 displays the DR-UV-Vis spectra of the samples whose XRD patterns are shown in Figure 7, as well as of a SnO_2 sample used as reference. At relatively short crystallisation times (1-3 days), there is not any indication of extraframework Sn, even in the highly crystalline samples (Figure 7). Therefore, almost complete tetrahedral incorporation of tin in crystalline Sn-Silicalite-1 is possible. After 6 days of crystallisation, part of the tin is still in tetrahedral coordination although most of them possesses higher coordination degree, suggesting that it has leached from the framework. Besides, the crystallinity of that sample decreases with regards the sample crystallised for 3 days (Figure 7). At longer crystallisation times (13 days), most of the tin is extra-framework and accordingly its crystallinity is even lower than that of the sample crystallised for 6 days. Figure 8 also list the tin content on each sample, measured by ICP-AES. It is noteworthy the increasing of the crystallization time leads to lower incorporation degrees of tin species into the zeolites, supporting the suggested tin leaching during prolonged crystallization times. Besides, no clear trend between crystallinity and tin content has been detected.

Figure 9 shows some SEM pictures of the 100 %-crystalline silicalite-1 obtained from a pure-SiO_2 xerogel, the samples Z2 (8% MFI) and Z3 (68 % MFI) obtained from SiO_2-SnO_2 xerogels gelified with NH_3 and the most crystalline sample transformed from SiO_2-SnO_2 xerogels gelified with TPAOH (sample Z6B). The particles forming the pure-silica sample posses almost-spherical morphology frequent in MFI materials, with a diameter of about 2 μm. The presence of tin almost does not change the morphology of the samples crystallised from TPAOH-gelified SiO_2-SnO_2 xerogels, excepting in the crystal size, what could suggest that the tin hinders the crystal growth process rather than the nucleation one. However, the shape of the particles is radically changed when the samples are obtained by the solid-state transformation of the NH_3-gelified xerogels. In these samples, the crystalline particles are parallelepipeds with a length larger than 15 μm and with a width of *ca.* 2 μm. It is a further indication of the different mechanism of crystallization followed by the NH_3 containing xerogels coming from the gelation step. Sample Z2 clearly contains crystalline and amorphous particles. Punctual EDX analyses, also shown in the table contained in Figure 9, evidence that the crystalline material is formed by Sn-poorer particles in comparison with the global tin content. It once again suggests that for this sample not only NH_3 as gelificant agent but also the presence of tin have negative effects on the kinetics of crystallisation of MFI phase. Besides, a table including the tin content measured by EDX for punctual analyses and by ICP-AES for bulk composition, has also been included for the samples analyzed by SEM.. The tin content found for sample Z6B, which is the most crystalline one, is almost that contained in the starting xerogel (Si/Sn molar ratio of 64) but the rest of the samples display lower tin content, evidencing the negative effect of the gelation of xerogels using ammonia instead of TPAOH in terms of both kinetics of zeolite transformation and tin incorporation.

Sn-silicalite from SiO_2-SnO_2 xerogels versus Sn-silicalite from conventional direct synthesis

As it was previously described, the heteroatom incorporation into zeolite framework through direct synthesis and solid-solid transformation of xerogels could not necessary follow the same mechanism [19],[20]. Consequently, the physico-chemical properties of both samples could be different. In order to deeply study these possible differences, we prepared a Sn-silicalite (called SnS-1 in this work) starting from a gel also containing 3 wt. % of Sn, rigorously following the most suitable method to produce Sn-silicalite-1 from direct crystallization amongst four different methods compared by Mal et al. [30]. The characterisation of this sample by different techniques was compared with that of the best Sn-

silicalite-1 prepared from xerogels SiO_2-SnO_2 (sample Z6B). ICP-AES analyses made clear that the tin content of the sample SnS-1 (0.86 wt. %) is less than one third of the metal content of the gel. In contrast, the zeolite Z6B contains 2.82 wt. % of tin content, almost 95% of the initial metal loading in the starting xerogels. Obviously, this meaningful difference evidences a much higher effectiveness of the tin incorporation into zeolites when prepared through transformation of xerogels into zeolites, compared with zeolites obtained by conventional procedure.

Figure 10 compares the XRD patterns and DR-UV-Vis spectra of both the as-made and calcined Sn-silicalite-1 samples prepared through the above mentioned methods. XRD patterns show that there is no significant difference in crystallinity between the SnS-1 and Z6B samples, either before or after calcination. In particular, the crystallinity was estimated as 95 % for as-made Z6B and 84 % for as-made SnS-1 with regards to the pure-silica MFI zeolite obtained from xerogel X0.

DR-UV-Vis spectroscopy shows key differences between both samples related to the tin coordination. Whereas the signals found in the spectra of sample Z6B can only be assigned to tetrahedral Sn coordination, extra signals at higher wavelengths (at *ca.* 250 nm) are found in the DR-UV-Vis spectrum of the sample SnS-1, indicating the presence of Sn in higher coordination number than four and therefore an undesirable Sn incorporation into the MFI framework [31]. Moreover, the calcination process seems to extract part of tin of the framework in both samples, but especially in calcined SnS-1 whose DR-UV-Vis spectrum shows a decrease of the signal attributed to tetrahedral contribution and a parallel increase of the signal centred at 250 nm. However, the changes in the DR-UV-Vis spectra of the sample Z6B, due to the calcination process, are less significant: Although there is an intensity increase of the contribution at wavelengths near 220 nm, this is generalised (including the tetrahedral contribution), and there is no significant changes further than 230 nm and the spectrum lacks a clear turning point. Such contribution at higher wavelengths, if really present, could be due to an increase of the tin coordination as a consequence of the hydration of the sample [12].

Figure 11A shows the NH_3-TPD plots of the calcined samples Z6B and SnS-1. Since the Sn(IV) incorporation into a SiO_2-based material does not generate any Brönsted acidity, the signal detected in the TPD plots must be attributed to some Lewis acidity related to such incorporation. The acidity is weak (the maximum intensity of the plot is found at *ca.* 110 ºC) and practically the same for both samples. However, the intensity of the signals suggests that

the efficiency of the tin incorporation has been higher into the sample prepared from xerogel. In order to qualitatively support this suggestion, the region of the FT-IR spectra shown in Figure 11B evidences a band at *ca.* 980 cm^{-1} in the spectrum of the sample Z6B almost not present in the sample SnS-1. In any case, admitting its existence in both spectra, the intensity of that band is much higher in the spectrum of the sample prepared from SiO_2-SnO_2 xerogels. As above-mentioned, although the origin of this band is still under discussion, it is generally taken as an indication of the heteroatom (Ti [32],[33], V [34], Cr [35], and even Sn itself [25]) incorporation into zeolite MFI framework. The lower frequency compared with the conventional band at 960 cm^{-1} related to the presence of Si-O-heteroatom bonds must be attributed to the chemical nature of tin. So far, this band has only been shown in a publication [36]. In some other publications, where the preparation of Sn-silicalite-1 was claimed by direct crystallization, such band was located in the IR spectra of the Sn-containing gels but not in that of the SnS-1 samples crystallised from them [25]. Even only a slight background perturbation rather than a well-defined band was the only indication in the IR spectrum of the Sn-beta [12], probably because of its low tin content. In addition, the T-O-T lattice vibration is clearly shifted towards lower values in the FT-IR spectrum of the sample Z6B, which would once again suggest a higher tin content into the framework of this sample [37].

Finally, in order to undoubtedly prove the incorporation of tin species into the MFI framework prepared for the transformation of SiO_2-SnO_2 xerogels, both samples were studied by ^{119}Sn MAS NMR spectroscopy (Figure 12). The ^{119}Sn spectra of tin-containing zeolites are dominted by a resonance band centred at ca. -707 ppm, which is slightly shifted toward high fields in comparison with the ^{119}Sn signal found in the spectrum of the xerogel X9, which has been included in Figure 12 for a better comparison. Of course, this shift indicates different tin environments in Sn-contining zeolites and in SiO_2-SnO_2 xerogels. Additionally, the NMR signal achieved for zeolite Z6B shows a narrower full width at half maximum (FWHM) than that found in the spectrum of the xerogel, which is in good agreement with a more homogeneous coordination of tin in zeolite Z6B. In other words, the isomorphic substitution of silicon atoms by tin species in uniform environments in zeolites lead to a narrowing of the ^{119}Sn MAS NMR signals.

More importantly, the ^{119}Sn MAS NMR spectrum of the sample SnS-1, prepared by the conventional hydrothermal method described by Ramaswamy et al. [30], shows two signals, one of them located at the same chemical shift at which tin oxide resonates, and the other one matching with that found for zeolite Z6B. This result, together with the studies by DR UV-

Vis and FTIR spectroscopies, allows us to conclude that the hydrothermal procedure leads zeolites showing dense phases of tin oxide as well as isolated tin species. In contrast, the direct transformation of SiO_2-SnO_2 xerogels into zeolites produces solely isolated tin species isomorphically substituting silicon atoms in the zeolite framework.

4. Conclusions

For the first time, the formation of Sn-zeolites starting from impregnated SiO_2-SnO_2 xerogels has been described. Two different Sn sources (anhydrous $SnCl_4$ and $SnCl_4 \cdot 5H_2O$), three different Sn contents (3, 6 and 9 wt. % of Sn) and two different gelation agents (NH_3 and TPAOH) were tested in the preparation of the xerogels. Minor differences between the physical-chemical properties of the xerogels prepared with different Sn sources were found though both of them possess certain Lewis acidity related to the incorporation of tin centres.

On the contrary, when crystallization of xerogels is attempted by wetness impregnation with aqueous TPAOH and subsequent hydrothermal treatment, those gelified with TPAOH led MFI-structured Sn-zeolite incorporating Sn into their framework. Proper tin containing zeolites were achieved in a narrow range of temperature and crystallization time. Meanwhile, the transformation of xerogels formed with ammonia as gelificant agent into zeolites is more kinetically disfavoured and the tin incorporation is of lower quality. The Sn-silicalite-1 sample prepared from xerogels gelified with TPAOH under the optimized hydrothermal conditions showed higher quality and efficiency in tin incorporation into zeolite framework than a Sn-silicalite-1 prepared by conventional direct method. FT-IR, DR-UV-vis and ^{119}Sn MAS NMR analyses confirmed the tetrahedral environment of the tin centres isomorphically substituting silicon atoms into the zeolite framework.

Acknowledgments

MSS acknowledges ‘Ministerio de Ciencia e Innovación’ of Spain for a ‘Ramón-y-Cajal’ contract.

References

[1] G.W. Skeeds, E.M. Flanigen, Stud. Surf. Sci. Catal. 49A (1989) 331.

[2] G.W. Skeeds, E.M. Flanigen, US Patent Appl. 133 (1987) 372

[3] N.K. Mal, V. Ramaswamy, S. Ganapathy, A.V. Ramswamy, Appl. Catal A: General 125 (1995) 233

[4] N.K. Mal, A.V. Ramaswamy, Chem. Commun. (1997) 425

[5] A. Corma, L.T. Nemeth, M. Renz, S. Valencia, Nature 412 (2001) 423

[6] A. Corma, M.T. Navarro, L. Nemeth, M. Renz, Chem. Commun. (2001) 2190

[7] U.R. Pillai, E. Shale-Demessie, J. Molec. Catal. A-Chem., 93 (2001) 191

[8] Z.Q. Lei, Q.H. Zhang, J.J. Luo, X.Y. He, Tetrahedron Lett. 46 (2005) 3505

[9] A. Corma, M.E. Domine, L. Nemeth, S. Valencia, J. Am. Chem. Soc. 124 (2002) 3194

[10] A. Corma, M.E. Domine, S. Valencia, J. Catal. 215 (2003) 294

[11] A. Corma, M. Renz, Chem. Commun (2004) 550

[12] M. Renz, T. Blasco, A. Corma, V. Fornés, R. Jensen, L Nemeth, Chem. Eur J. **8**, (2002) 4708

[13] S. Shetty, S. Pal, D.G. Kanhere, A. Goursot, Chem. A Eur. J. **12**, (2006) 518

[14] T. Tatsumi, M. Nakamura, S. Negeshi, H. Tominaga, J. Chem. Soc, Chem. Commun. (1990) 476

[15] D.R.C. Huybrechts, P. Buskens, P.A. Jacobs, J. Mol. Catal. **71**, (1992) 129

[16] A. Tuel, Y. Bentaarit, Zeolites 14 (1994) 594

[17] J.E. Gallot, D.T. On, M.P. Kapoor, S. Kaliaguine, Ind. Eng. Chem. Res. **36** (1997) 3458

[18] M.A. Uguina, D.P. Serrano, G. Ovejero, R. van Grieken, M. Camacho, Appl. Catal. A: Gen **124** (1995) 391

[19] D.P. Serrano, M.A. Uguina, G. Ovejero, R. van Grieken, M. Camacho, Chem. Commun. (1996) 1097

[20] D.P. Serrano, M.A. Uguina, G. Ovejero, R. van Grieken, M. Camacho, Microp. Mater. **7** (1996) 309

[21] C. Canevali, N. Chiodini, F. Morazzoni, J. Padovani, A. Paleari, R. Scotti, G. Spinolo, J. Non-Crystall. Solids **293** (2001) 32

[22] G. Mountjoy, D.M. Pickup, G.W. Wallidge, R. Anderson, J.M. Cole, R.J. Newport, M.E. Smith, Chem. Mater. 11, (1999) 1253

[23] N.K. Mal, A. Bhaumik, R. Kumar, A. V. Ramaswamy, Catal. Lett. **33** (1995) 387

[24] S.P. Naik, J.C. Chen, A.S.T. Chiang, Microp. Mesop. Mater. 54 (2002) 293

[25] P. Fejes, J.B. Nagy, K. Kovács, G. Vankó, Appl. Catal. A:Gen 145 (1996) 155

[26] K. Chaudhari, T.K. Das, P.R. Rajmohanan, K. Lazar, S. Sivasanker, A.J. Chandwadkar, J. Catal. **183** (1999) 281

[27] G. Ricchiardi, A. Damin, S. Bordiga, C. Lambert, G. Spano, F. Rivetti, A. Zecchina, J. Am. Chem. Soc. 123 (2001) 11409

[28] M.A. Camblor, A. Corma, J. Perez-Pariente, J. Chem. Soc., Chem. Commun. (1993) 557

[29] M. Boronat, P. Concepcion, A. Corma, M. Renz, S. Valencia, J. Catal. 234 (2005) 111

[30] N.K. Mal, V. Ramaswamy, P.R. Rajomohanan, A. V. Ramaswamy, Microp. Mater. 12 (1997) 331

[31] N.K. Mal, A.V. Ramaswamy, J. Mol. Catal. A: Chem. 105 (1996) 149

[32] E. Astorino, J.B. Peri, R.J. Willey, G. Busca, J. Catal. 157 (1995) 482

[33] B. Sulikowski, J. Klinowski, Appl. Catal. A 84 (1992) 141

[34] P.R. Hari Prasad Rao, R. Kumar, A.V. Ramaswamy and P. Ratnasamy, Zeolites 13 (1993) 663

[35] T. Chapus, A. Tuel, Y. Ben Taarit, C. Naccache, Zeolites, 14 (1994) 349

[36] N.K. Mal, A. Bhaumik, V. Ramaswamy, A.A. Belhekar, A.V. Ramaswamy, Stud. Surf. Sci. Catal. 94 (1994) 317

[37] N.K. Mal, V. Ramaswamy, S. Ganapathy, A. V. Ramaswamy, J. Chem. Soc., Chem. Commun. (1994) 1933

Figure Captions

Figure 1. DR-UV-Vis spectra of xerogels prepared from anhydrous $SnCl_4$ or $SnCl_4 \cdot 5H_2O$ as Sn source and with 3, 6 or 9 wt. % of Sn

Figure 2. ^{119}Sn MAS NMR spectra of xerogels SiO_2-SnO_2 with 3 and 9 wt. % of Sn. The ^{119}Sn spectra of SnO_2 is also shown for comparison. * denotes spin-side bands in the spectrum of SnO_2

Figure 3. A) FT-IR spectra of the SiO_2-SnO_2 xerogels containing 0, 3, 6 and 9 wt. % of Sn and prepared with NH_3 as gelificant agent. Arrows point out the bands discussed in the text and whose frequencies are also indicated. B) TGA curves of the same samples. Weight loss (straight lines, left Y-axis) and its derivative (dashed lines, right Y-axis) are plotted.

Figure 4. NH_3-TPD- plots of the xerogels X0, X3 and X9

Figure 5. A) DR-UV-Vis spectra of SiO_2-SnO_2 xerogels with 3 wt. % of Sn prepared with NH_3 (black) and TPAOH (red). B) TGA curves of the same samples. Weight loss (solid lines, left Y-axis) and its derivative (dashed lines, right Y-axis) are plotted.

Figure 6. A) XRD patterns of the solids Z1, Z2 and Z3 resulting from the hydrothermal treatment at 150, 170 and 190 ºC, respectively, for 13 days of TPAOH-impregnated SiO_2-SnO_2 xerogels gelified with NH_3. B) DR-UV-Vis spectra of the same samples

Figure 7. A) XRD patterns of the samples crystallised from the hydrothermal treatment at 170 ºC for the indicated crystallisation times of a TPAOH-impregnated SiO_2-SnO_2 xerogel with 3 wt % of Sn prepared from $SnCl_4 \cdot 5H_2O$ and gelified with TPAOH. B) Plot of MFI crystallinity of XRD patterns of Figure 7A *vs.* crystallisation time.

Figure 8. DR-UV-Vis spectra of the samples crystallised from the hydrothermal treatment at 170 ºC for the indicated crystallisation times of a TPAOH-impregnated SiO_2-SnO_2 xerogel with 3 wt % of Sn prepared with $SnCl_4 \cdot 5H_2O$ and gelified with TPAOH

Figure 9. SEM pictures of a Sn-free silicalite (from xerogel X0), of the semi-crystalline sample Z2, of the two crystalline SnS-1 samples: sample Z3 obtained starting from the

xerogel X3 gelified with ammonia and sample Z6B crystallised from a xerogel SiO_2-SnO_2 gelified with TPAOH. Data of some punctual and global EDX analyses are also shown

Figure 10. A) XRD patterns of the as-prepared and calcined samples Z6B and SnS-1. B) 200 – 300 nm region of the DR-UV-Vis spectra of the same samples.

Figure 11. A) NH_3-TPD plots of the calcined samples Z6B and SnS-1. B) 700-1200 cm^{-1} region of the FT-IR spectra of the as-prepared samples Z6B and SnS-1

Figure 12. ^{119}Sn MAS NMR spectra recorded for Sn-containing materials with different metal environments.

Table 1. Nature of starting xerogel, hydrothermal conditions and MFI cristallinity of some relevant attempts to transform xerogels SiO_2-SnO_2 into Sn-sillicalite-1.[a]

Sample	Starting xerogel		Hydrothermal treatment		Phases
	$SnCl_4$ source	**Gelificant agent**	**T / ºC**	**t / days**	**% MFI** [b]
Z1	$\cdot 5H_2O$	NH_3	150	13	5
Z2 [c]	$\cdot 5H_2O$	NH_3	170	13	8
Z3	$\cdot 5H_2O$	NH_3	190	13	68
Z4	anhydrous	NH_3	190	13	9
Z2 [c]	$\cdot 5H_2O$	NH_3	170	13	8
Z5	$\cdot 5H_2O$	TPAOH	170	13	57

[a] For clarity, on every compared set of experiments, the changed parameters are on grey background; [b] Calculated from XRD; [c] Sample Z2 is repeated to facilitate comparison.

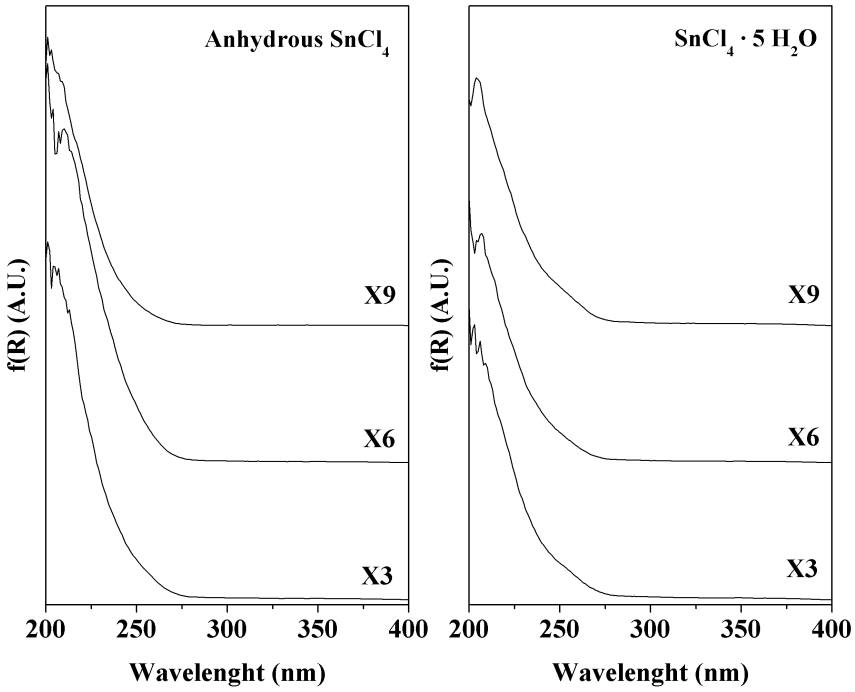
Anhydrous SnCl4
SnCl4 · 5 H2O
f(R) (A.U.)
X9
X6
X3
200
250
300
350
400
Wavelenght (nm)

Figure 1

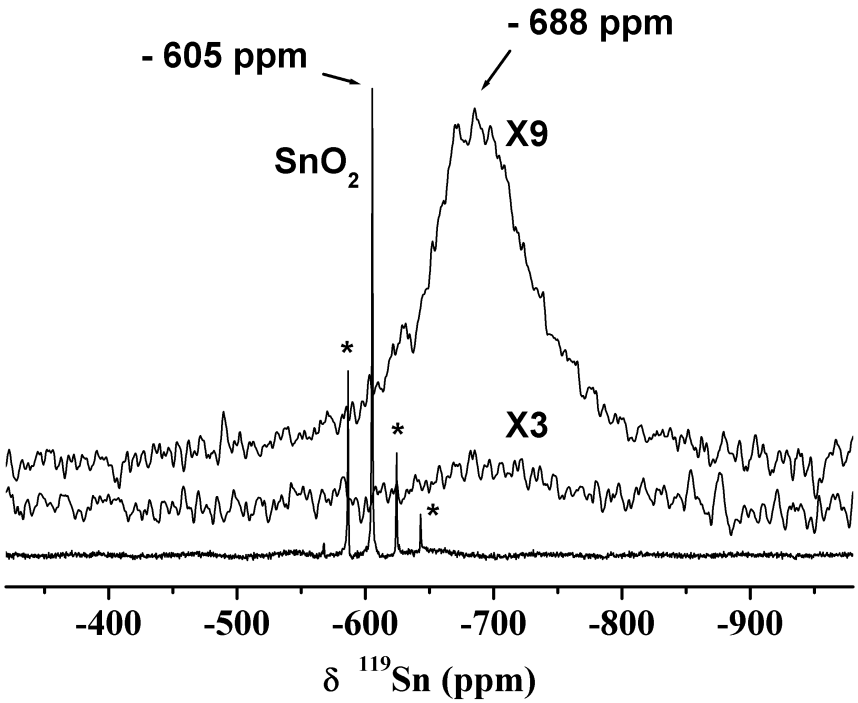

Figure 2

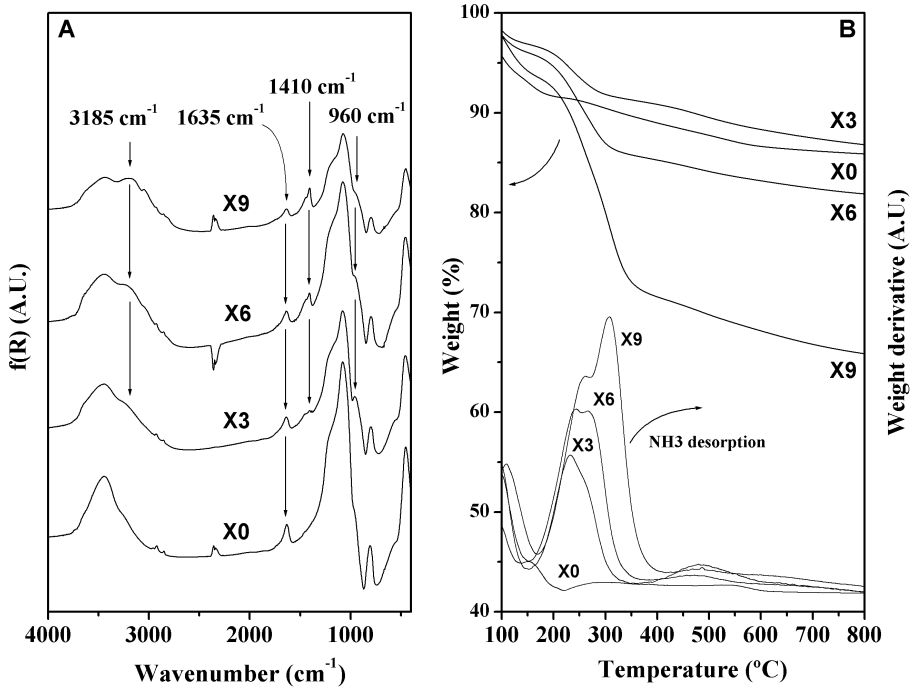
A
3185 cm-1
1635 cm-1
1410 cm-1
960 cm-1
X9
X6
X3
X0
f(R) (A.U.)
4000
3000
2000
1000
Wavenumber (cm-1)
B
X3
X0
X6
X9
X9
X6
X3
X0
NH3 desorption
Weight (%)
Weight derivative (A.U.)
100
90
80
70
60
50
40
100
200
300
400
500
600
700
800
Temperature (°C)

Figure 3

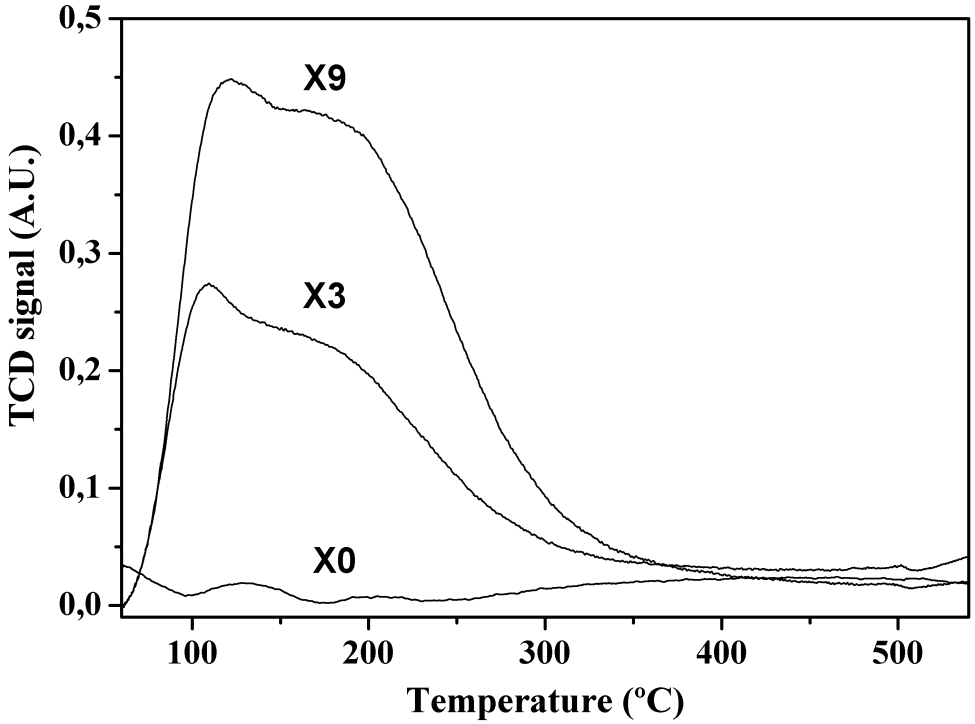
0,5
0,4
0,3
0,2
0,1
0,0
TCD signal (A.U.)
X9
X3
X0
100
200
300
400
500
Temperature (°C)

Figure 4

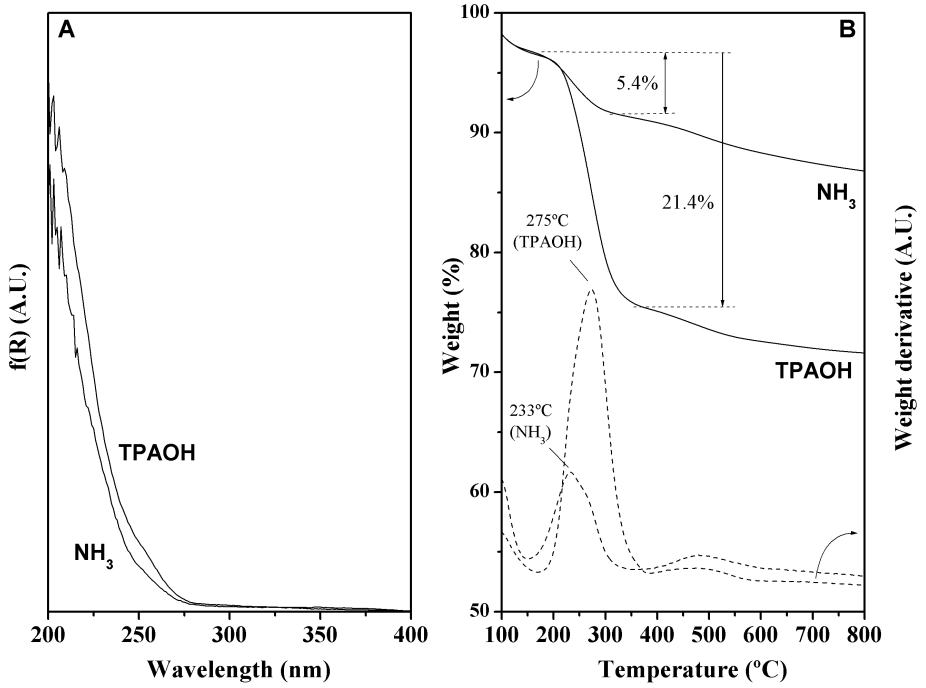
A
f(R) (A.U.)
TPAOH
NH3
200
250
300
350
400
Wavelength (nm)
B
100
90
80
70
60
50
Weight (%)
5.4%
21.4%
NH3
TPAOH
275°C
(TPAOH)
233°C
(NH3)
100
200
300
400
500
600
700
800
Temperature (°C)
Weight derivative (A.U.)

Figure 5

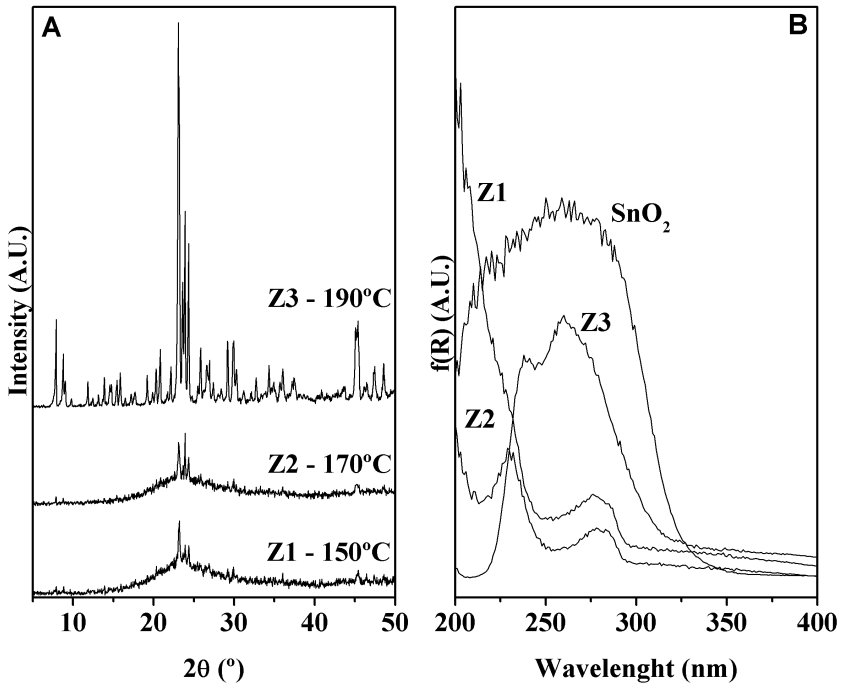
A
Intensity (A.U.)
Z3 - 190ºC
Z2 - 170ºC
Z1 - 150ºC
10
20
30
40
50
2θ (º)
B
f(R) (A.U.)
Z1
SnO2
Z3
Z2
200
250
300
350
400
Wavelenght (nm)

Figure 6

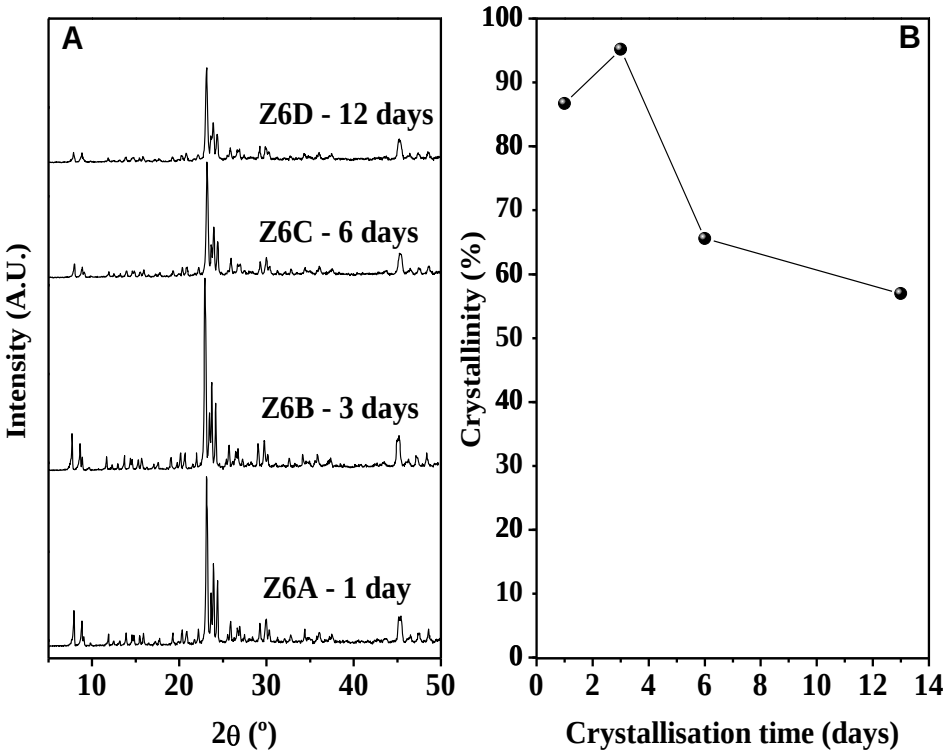
A
Z6D - 12 days
Z6C - 6 days
Z6B - 3 days
Z6A - 1 day
Intensity (A.U.)
10
20
30
40
50
2θ (º)
B
Crystallinity (%)
0
10
20
30
40
50
60
70
80
90
100
0
2
4
6
8
10
12
14
Crystallisation time (days)

Figure 7

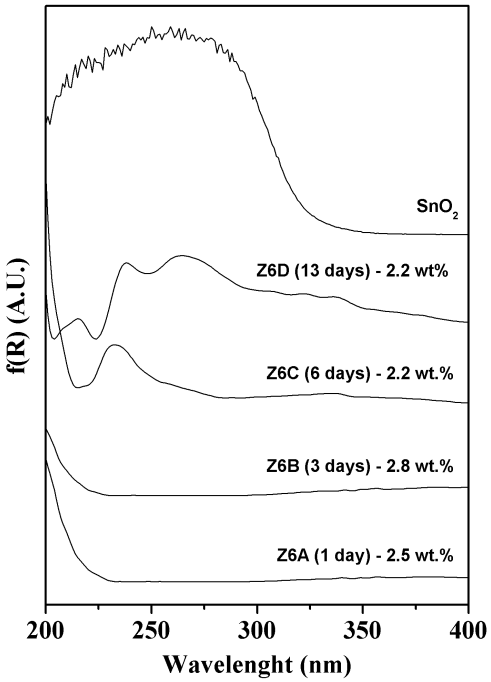
SnO2
Z6D (13 days) - 2.2 wt%
Z6C (6 days) - 2.2 wt.%
Z6B (3 days) - 2.8 wt.%
Z6A (1 day) - 2.5 wt.%
f(R) (A.U.)
200
250
300
350
400
Wavelenght (nm)

Figure 8

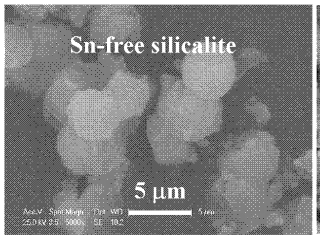

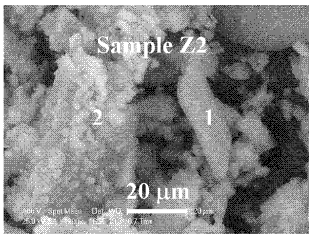

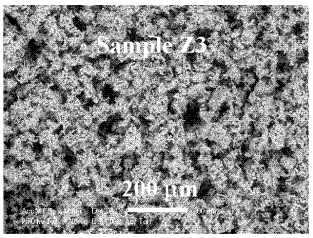

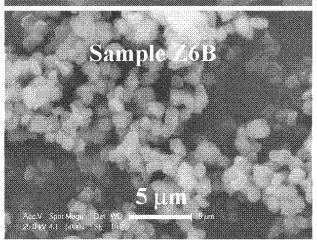

Chemical Analyses

Sample	Sn (wt.%)	Si/Sn
Z2 #1 *	1.7	114
Z2 #2 *	0.9	217
Z2 global	1.6	120
Z3 global	1.4	140
Z6B global	2.8	68

* EDS analyses

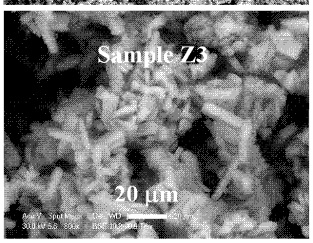

Figure 9

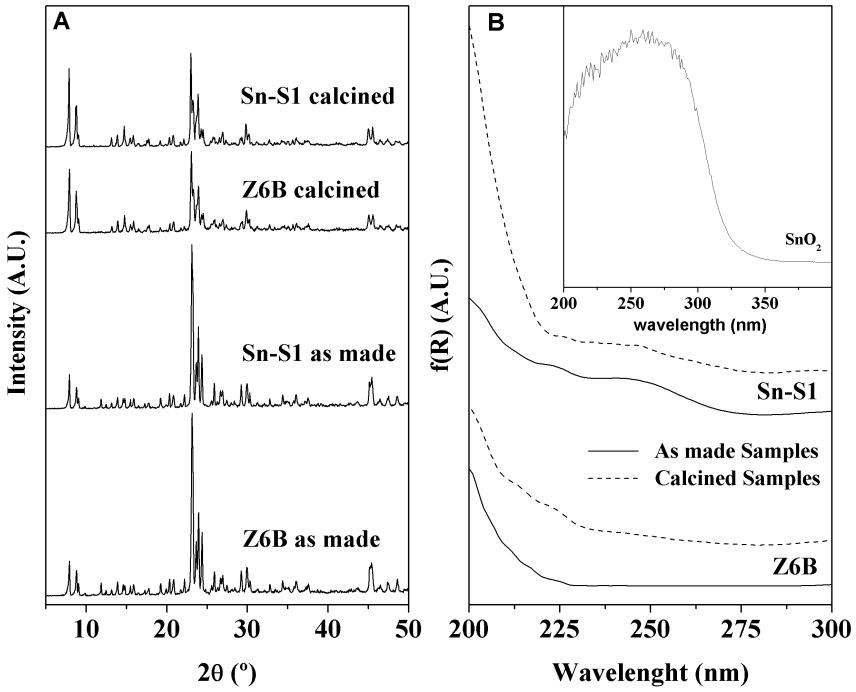
A
Sn-S1 calcined
Z6B calcined
Sn-S1 as made
Z6B as made
Intensity (A.U.)
10
20
30
40
50
2θ (º)
B
f(R) (A.U.)
SnO2
200
250
300
350
wavelength (nm)
Sn-S1
As made Samples
Calcined Samples
Z6B
200
225
250
275
300
Wavelenght (nm)

Figure 10

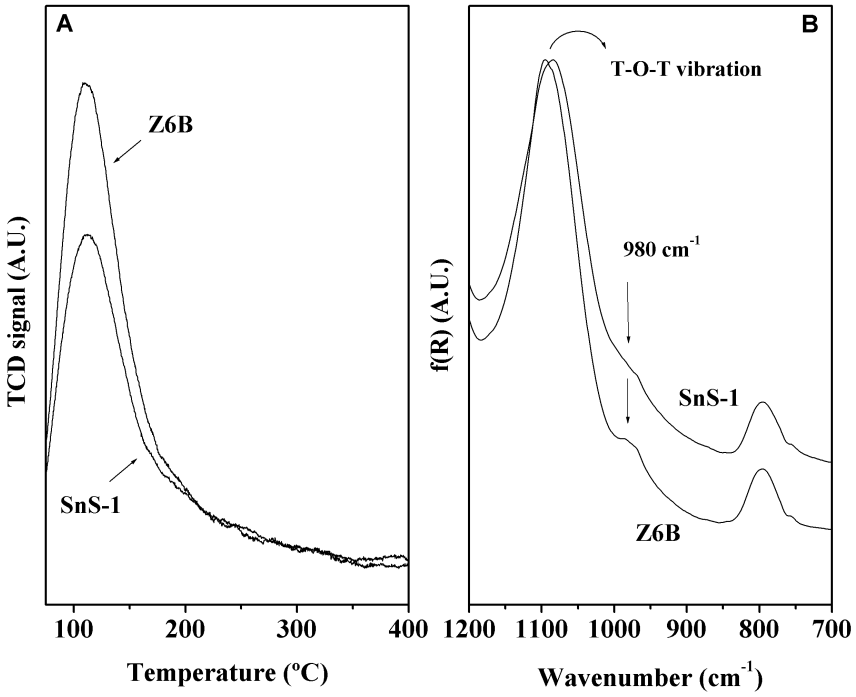
A
Z6B
SnS-1
TCD signal (A.U.)
100
200
300
400
Temperature (ºC)
B
T-O-T vibration
980 cm-1
SnS-1
Z6B
f(R) (A.U.)
1200
1100
1000
900
800
700
Wavenumber (cm-1)

Figure 11

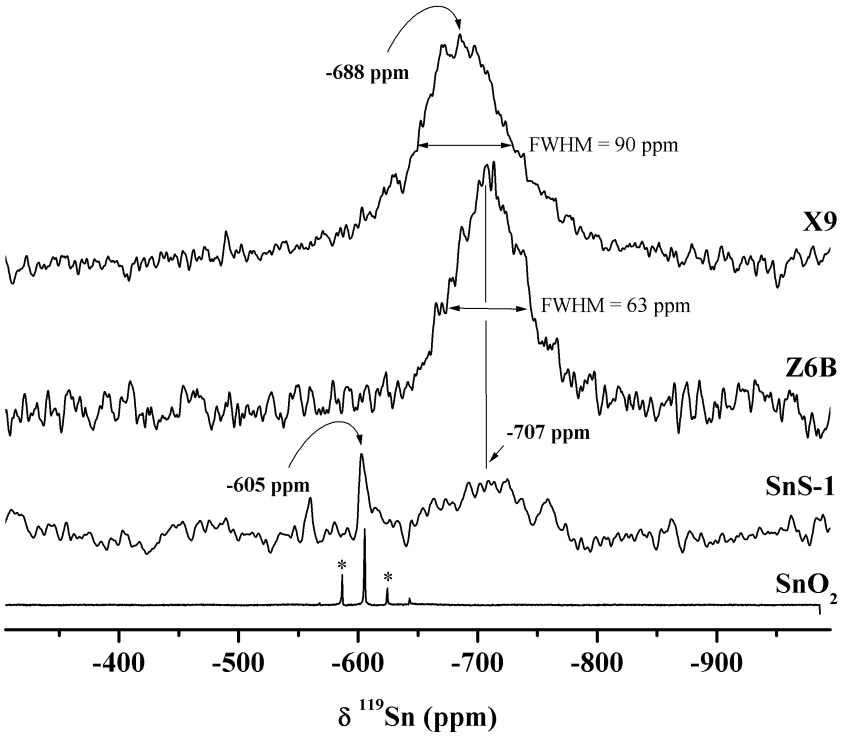
-688 ppm
FWHM = 90 ppm
X9
FWHM = 63 ppm
Z6B
-707 ppm
-605 ppm
SnS-1
*
*
SnO2
-400
-500
-600
-700
-800
-900
δ 119Sn (ppm)

Figure 12